

Direct observation of ionic aggregates in sulphonated polystyrene ionomers

Chi Li*, Richard A. Register and Stuart L. Cooper†

Department of Chemical Engineering, University of Wisconsin at Madison, Madison, WI 53706, USA

(Received 25 July 1988; revised 26 September 1988; accepted 6 October 1988)

Applications of electron microscopy to ionomers have not generally been successful in the past, due to the small size of the ionic aggregates and their irregular distribution throughout the polymer matrix. Ionic domains were observed in samples of Zn^{2+} and Ni^{2+} neutralized sulphonated polystyrene (SPS), at sulphonation levels of 1.68 mol% and 3.37 mol%, using high-voltage (1.0 MeV) electron microscopy (HVEM). The specimens were solvent-cast films which contained suitable 'thin spots' only a few interaggregate dimensions thick. The observed contrast is not due to phase grain artifact, as demonstrated by a through-focus series of micrographs of the Zn^{2+} ionomer and polystyrene homopolymer. Contrast was observed only in the former case. The aggregates are approximately spherical and roughly 3 nm in diameter, and appear identical for both Ni^{2+} and Zn^{2+} materials. However, Cs^+ neutralized SPS exhibited no ionic aggregates. This is probably due to the rapid rate of solvent evaporation coupled with the weaker coulombic forces in the Cs^+ neutralized material, both of which hinder the formation of ionic aggregates.

(Keywords: ionomer; lightly sulphonated polystyrene; ionic aggregate; transmission electron microscopy (TEM); high-voltage electron microscopy (HVEM))

INTRODUCTION

Over the past two decades, incorporation of ionizable groups into a polymer has become an important means of obtaining desired physical properties in a high-performance material. Although these materials, termed ionomers, contain only 10% or less of ionic comonomer, the ionic groups have a major effect on material properties. For example, the electrolyte transport properties can be dramatically enhanced, while in addition marked increases in modulus, adhesive strength, tear resistance, melt viscosity, oil resistance, glass transition temperature, abrasion resistance, and impact strength can also be achieved¹. It has been proposed², and by now generally accepted, that these effects result from aggregation of the ions into microdomains, which act as physical crosslinks in the material.

The qualitative explanation that the ionic groups aggregate, and thereby alter the behaviour of the material, is only a start towards understanding ionomers. Before being able to create a material with a desired set of physical properties, it is essential to understand ionomer morphology and how it controls those properties. In general, transmission electron microscopy (TEM) has been very useful in characterizing the morphology of polymers, but due to the small size of the ionic aggregates, it has made little impact thus far in the study of ionomers. Instead, ionomer morphology has been probed primarily by the small-angle scattering of X-rays³⁻¹⁵ (SAXS) and neutrons¹⁵⁻¹⁸ (SANS). While these investigations have revealed much regarding the structure of ionomers, interpretation of the scattering data is model-dependent,

and there is still disagreement over the correct model. Some workers have ascribed the observed scattering peak to an interference between ionic aggregates⁷, while others have claimed that it results from intraparticle scattering from aggregates with a spherical^{4,13} or lamellar⁵ core-shell morphology. The application of these models to SAXS data has been examined by Yarusso and Cooper⁷. The scattering from semicrystalline ionomers such as ethylene/methacrylic acid salts and perfluorinated ionomer membranes is further complicated by scattering from the crystallites. Clearly, direct visualization of the ionic domains would be invaluable in interpreting the large body of scattering data in the literature.

Handlin *et al.*¹⁹ have critically reviewed previous applications of transmission electron microscopy (TEM) to ionomers. As they point out, a major difficulty lies in obtaining a sample thin enough that its TEM projection is interpretable. This situation is shown schematically in *Figure 1*. For materials which have a lattice-type arrangement of the ionic microdomains, it is possible to select a particular direction of observation such that constructive reinforcement of the amplitude contrast between the two phases gives rise to an interpretable image, even though the sample may be many domain spacings in thickness. This fact has enabled the routine observation of microdomains in narrow polydispersity block copolymers²⁰ where one phase is stainable with a heavy metal, such as those of styrene and butadiene. Graiver *et al.*^{21,22} have observed a regular lamellar morphology in polysiloxane zwitterionomers, where the ionic domains were stained with uranyl acetate. More recently, Feng and coworkers²³ have observed a regular morphology in segmented ionenes, using only the inherent contrast between the ionic and nonionic domains.

However, typical ionomers are not expected to possess

* Present address: Scientific Research Staff, Ford Motor Company, Dearborn, MI 48121, USA

† To whom correspondence should be addressed

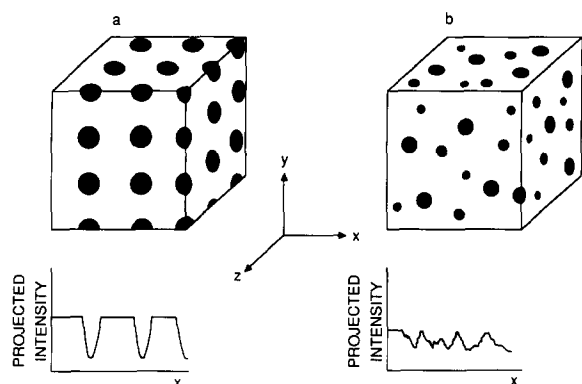


Figure 1 Possible arrangements of monodisperse spherical microdomains in a matrix. (a) Lattice-type arrangements of the microdomains lead to defined projections through the samples; (b) irregular arrangements cause destructive interference of the amplitude contrast, and no defined projection. Note that even though the microdomains are monodisperse in both cases, the irregular arrangement in (b) causes the loci of intersection of any given plane with the domains to be circles of various sizes

a regular lattice-type arrangement of the ionic aggregates, as evidenced by the single broad maximum which is usually observed in SAXS and SANS. The particle spacings are expected to be on the order of 2–10 nm, based on SAXS and SANS experiments and using an interparticle scattering model⁷. Thus, a sample film for TEM must be no more than a few times this thickness or the projection will be featureless, as shown in *Figure 1b*. Moreover, Handlin *et al.*^{19,24} point out that because such thin sections have not been used in the past, the ‘features’ that other investigators have observed at this size scale^{13,25–27} arise from phase grain artifacts due to defocusing. To confirm this conclusion, they investigated the caesium salts of ethylene/methacrylic acid, sulphonated polystyrene, sulphonated polybutadiene, and sulphonated EPDM (ethylene-propylene-diene rubber). The only non-artifactual image they were able to observe was of large (100 nm) dark regions in sulphonated EPDM. Similar features have also been observed by Agarwal and Prestridge²⁸ in sulphonated EPDM and by Clough *et al.*¹⁸ in osmium tetroxide-stained ampholytic styrene ionomers. While their origin is not yet clear, these features are far too large to account for the observed scattering peak, and thus are not the fundamental ‘ionic aggregates’. Moreover, the absence of such features in the other ionomers suggests that they are peculiar to the two ionomers in which they have been observed, rather than being a general feature.

A related study was performed by Pinéri, Meyer, and Bourret^{29,30} on a ferric complex of a butadiene–styrene–vinylpyridine random terpolymer. Using TEM, they observed a wide size distribution of iron-containing particles, ranging from 0.5 to 150 nm. The same materials were also investigated by SAXS, SANS, and Mössbauer spectroscopy, all of which generally confirmed the existence of aggregates having, for the most part, diameters less than 10 nm. The existence of some extremely large aggregates is surprising, because the necessary attachment of polymer chains to the ionic sites would be expected to limit the maximum cluster size. Therefore, these observations may be peculiar to this material. It should be noted that this material is not an ionomer in the usual sense, as the polymer chain does not contain bound ionic functionality.

In addition to the difficulty in preparing sufficiently thin samples, and in discriminating between the true sample morphology (amplitude contrast) and artifacts due to defocusing (phase contrast), there are two other impediments regarding the application of TEM to ionomers. First, the extremely small size of the domains mandates the use of a microscope having a resolution of a few tenths of a nanometre. Second, the sample can suffer damage in the electron beam, causing mass loss and morphological changes. While beam damage is a general problem when using TEM to study polymers, it is especially severe in the study of ionomers, because the high magnifications required necessarily mean high beam current densities.

Two developments in TEM can mitigate these problems, however. High-voltage electron microscopes (HVEM) operated at 1 MeV accelerating potential provide both a nominal resolution of 0.3 nm and significantly reduced beam damage when compared with a typical 100 keV TEM, such as that used by Handlin *et al.*^{19,24}. Digital image processing and enhancement can also be employed in TEM, to reduce the exposure of the sample to the electron beam and minimize beam damage. In light of these recent developments, and considering the benefits of direct observation of ionomer morphology, a renewed investigation of ionomers by HVEM was undertaken. Because it is free from possible complications due to crystallinity, and because it is soluble at room temperature in a variety of mixed solvents, we chose to examine lightly sulphonated polystyrene (SPS), at varying sulphonation levels and with various neutralizing cations.

EXPERIMENTAL

Sample preparation

The sulphonated polystyrene studied was obtained from Dr Robert Lundberg and the late Dr Henry Makowski of the Exxon Research and Engineering Company, and was prepared by a post-polymerization sulphonation of the base polystyrene to place sulphonic acid groups at the *para* positions of the benzene rings. The detailed synthetic procedure has been presented previously³¹. The product has been shown to possess a random distribution of styrene sulphonic acid repeat units, and the reaction proceeds with little³² or no³³ alteration of the molecular weight or molecular weight distribution.

The samples used in this study contained 1.68 and 3.37 mol% sulphonated styrene repeat units, as determined by atomic absorption analysis. Relatively low sulphonation levels were chosen so as to decrease the number density of ionic aggregates and thus mitigate the domain overlap problem discussed above. These materials in the neutralized state have been shown by SAXS to contain ionic aggregates⁷. Dilute (0.2 wt%) solutions of the neutralized ionomers in dimethyl sulphoxide/mixed xylenes (50/50 v/v) were prepared by first dissolving the appropriate amount of acid SPS in the solvent mixture and then adding the appropriate amount of neutralizing agent, in methanol solution (5–10 wt%), to neutralize 85% of the sulphonic acid groups. No visible change in the clarity of the solution occurred upon neutralization. The neutralizing agents used were nickel acetate tetrahydrate (Alfa), zinc acetate dihydrate (Mallinckrodt, AR) and anhydrous caesium acetate (Aldrich, 98%).

To prepare extremely thin films of SPS, a drop of the SPS solution was cast directly onto a 500 mesh copper TEM grid. The excess solution was removed by absorption into a low dust laboratory wipe and the grid placed under a 75 W incandescent heat source to rapidly dry the specimen. Further solvent evaporation was achieved in a vacuum oven at 60°C for 48 h. Although the films produced by this technique are not of uniform thickness, and indeed do not cover most of the grid openings, they are sufficiently thin in spots to provide minimal domain overlap. Attempts to microtome bulk specimens of SPS have thus far proven unsuccessful, due to the ultrathin samples required.

We followed the same procedure in producing specimens of the acid form of SPS (3.37 mol% sulphonation) and of atactic polystyrene homopolymer (Aldrich, M_w 250 000), except that no neutralizing agent was required. Comparison of micrographs of these specimens with those of the neutralized SPS specimens under identical microscope conditions permits the identification of defocusing artifacts.

HVEM description

The HVEM was an AEI EM-7 Mk 11 HVEM operated at 1.0 MeV with 10 or 30 μm objective apertures for a resolution of 0.3 nm or better at magnifications up to 316 000. In addition to photographic recording, the HVEM is also equipped with a high sensitivity video camera and a digital image processor. The sensitivity of the video camera allows specimen viewing and focusing at very low beam current, sharply reducing beam damage to the sample. Extreme care was taken to minimize the exposure of the sample to the electron beam. No morphological changes were observed during focusing. Kodak 4199 high contrast film was used for image recording. A detailed description of the HVEM may be found in the literature³⁴.

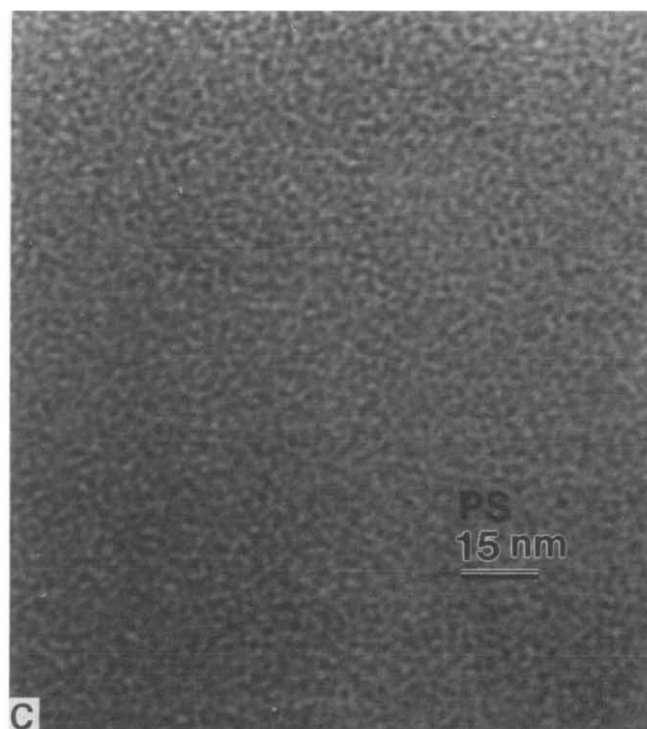
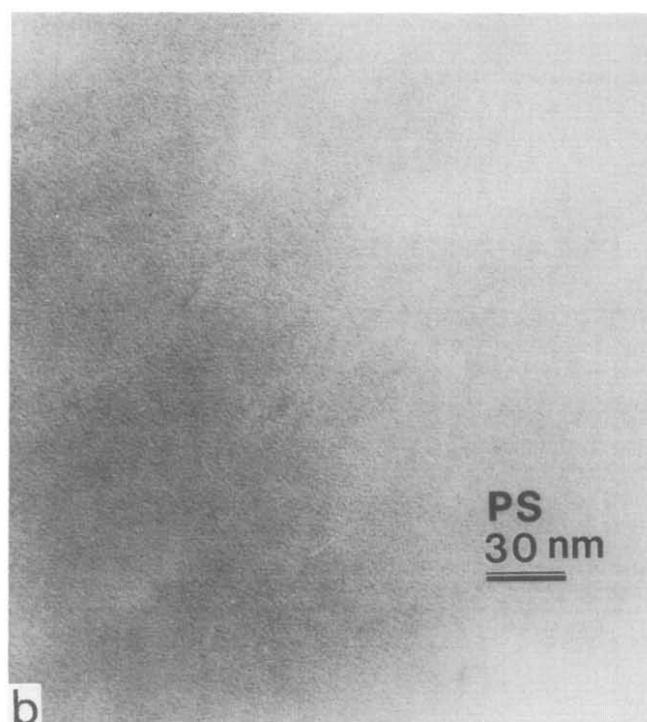
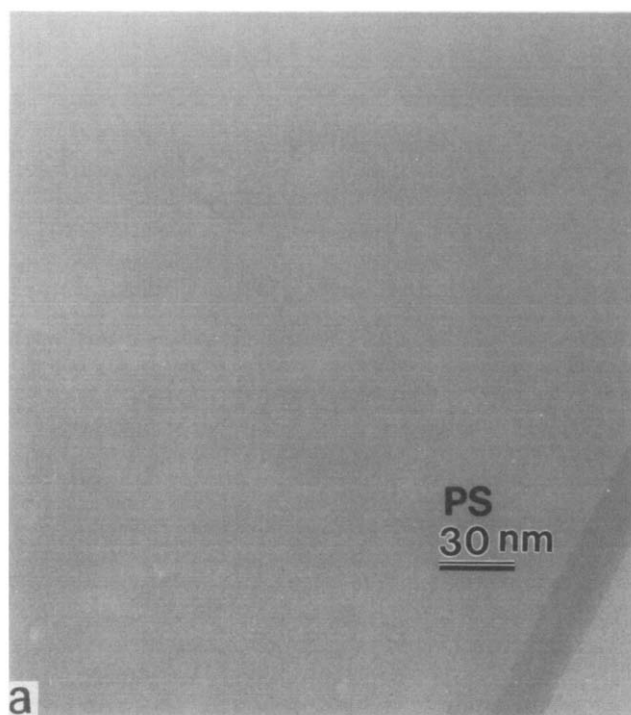


Figure 2 Polystyrene homopolymer, 30 μm aperture. (a) Critical focus; (b) 40 nm under focus; (c) 1400 nm under focus. Band visible in lower right corner in part (a) is the edge of the film

RESULTS

The first specimen examined was atactic polystyrene homopolymer, which should exhibit no microphase separation. To observe the effect of defocusing on the sample image, micrographs were taken at critical focus (focus in the plane of the sample, *Figure 2a*), at 4 nm under focus (focus 4 nm above the plane of the sample, *Figure 2b*), and at 1400 nm under focus (*Figure 2c*). The dark band observed in *Figure 2a* is the edge of the film, which aids in focusing. No other features can be observed. In contrast, *Figure 2b* shows the commonly observed 'salt and pepper

pattern', with a size scale of approximately 0.5 nm. This nodular pattern is due to selective amplification of thermal density fluctuations of a particular wavelength by the microscope transfer function and is known as phase contrast²⁴. Such a pattern does not reflect microphase separation in the sample. A similar pattern can be seen in *Figure 2c*, where the size of the nodules has increased to approximately 1.5 nm due to the larger defocus.

There is some question as to whether aggregates are present in the acid form of SPS. One study on compression moulded specimens⁷ showed that the SAXS peak was present for acid contents as low as 1.68 mol%. Another study, also on compression moulded specimens⁹, found a SAXS peak at 11.5 mol% sulphonation but no peak at 5.5 mol%. It has also been demonstrated^{10,14} that casting from solvent tends to inhibit aggregate formation in SPS ionomers, when compared with compression moulding. *Figure 3* shows the micrograph for the acid form of SPS. Again, the line running through the image is the edge of the specimen. No microphase separation is observed here. However, the amplitude contrast between any aggregates in the acid SPS and the polystyrene matrix (due primarily to the sulphonic acid groups) would be expected to be rather small, so the featureless micrograph does not definitively rule out aggregation of the acid groups. The contrast would be expected to be much larger when the acid groups are neutralized with a metal salt. *Figure 4* shows the micrographs for the Zn²⁺ salt of SPS with 3.37 mol% ionic groups, and here microphase separation is clearly evident. A 30 μm objective aperture was used to record these micrographs, and the focus was changed to rule out the possibility of the observed structure being due to phase contrast. While the apparent contrast between the ionic microdomains and the matrix changes as the focus is changed from 20 000 nm over focus, through critical, to 500 nm under focus, the observed structure

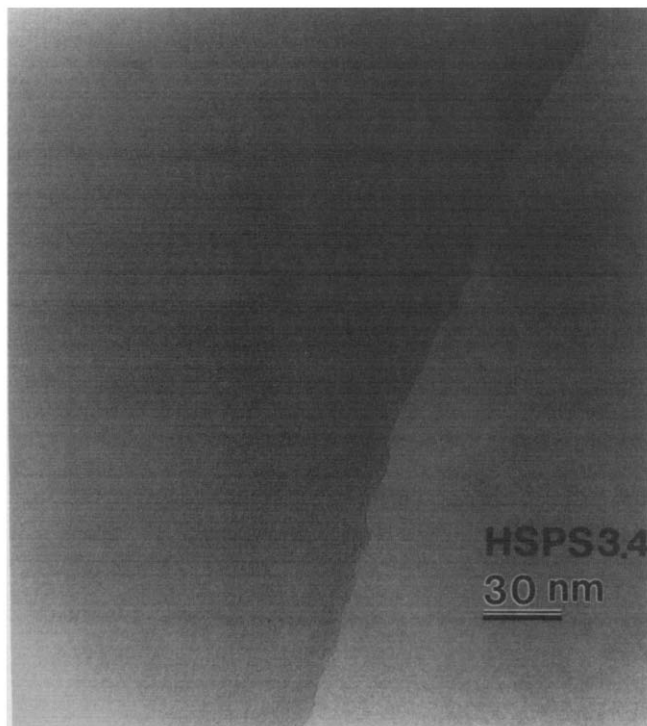


Figure 3 Acid SPS, 3.37 mol% sulphonation, 30 μm aperture, critical focus. The line running from top to bottom is the edge of the film; specimen is to the left

does not change. This confirms that the observed structure is due to microphase separation. Note that, based on the previous work of Yarusso and Cooper⁷, the electron density difference between the aggregates and the matrix is expected to be about 150 nm⁻³. The electron density of pure polystyrene is approximately 340 nm⁻³ at r.t. Thus, sufficient aggregate–matrix contrast should exist to observe the ionic aggregates. However, recent reevaluation of the SAXS data presented in reference 7 indicates that the absolute intensities used were too low by a factor of 2.88. This error translates directly into the square of the electron density difference, hence the value of 150 nm⁻³ given here.

To examine the effects of counter ion type and ion concentration, the next samples studied were 3.37 mol% SPS neutralized with Ni²⁺ and 1.68 mol% SPS neutralized with Zn²⁺. To improve the apparent aggregate–matrix contrast, a 10 μm objective aperture was used (compared to the 30 μm aperture used in *Figures 2–4*) and the magnification was more than doubled to facilitate measurement of the sizes of the aggregates. Except for *Figures 2* and *4*, all micrographs shown were taken at critical focus. *Figure 5* reveals the presence of numerous dark regions representing the ionic aggregates in the Ni²⁺ neutralized 3.37 mol% SPS. There appears to be a considerable distribution of sizes, although some of the larger regions may be due to partial overlap of two or more smaller aggregates in the line of projection. Those spots which clearly are not the result of overlap appear to be approximately 3 nm in diameter. The stacking problem, though minimized here, makes it difficult to use digital image analysis to determine the average and distribution of aggregate diameters. Moreover, the unknown and nonuniform thickness of the film prohibits the determination of interaggregate spacings or the number density of ionic aggregates.

Figure 6 shows the Zn²⁺ salt of the 1.68 mol% SPS. The blank region in the lower right corner of the micrograph is beyond the edge of the specimen. The aggregates here appear similar to those observed in the previous micrograph for the Ni²⁺ salt of the 3.37 mol% SPS, taken under identical conditions. Finally, *Figure 7* shows the micrograph of the Cs⁺ salt of the 1.68 mol% SPS, taken under the same conditions as *Figure 4c* (lower magnification, 30 μm aperture, critical focus). The edge of the specimen can be clearly seen running through the micrograph, with the darker region to the left being the sample. Quite surprisingly, no ionic aggregates can be observed, while they were clearly visible for the analogous Zn²⁺ sample in *Figure 4c*. This point will be discussed below.

DISCUSSION

The micrographs in *Figures 4–6* clearly show a morphology which consists of roughly spherical ionic aggregates embedded in a polymer matrix, consistent with several previous models. As reviewed by Yarusso and Cooper⁷, both the interparticle and intraparticle models, when fit to SAXS data for Zn²⁺ salts of SPS, give an aggregate diameter of approximately 2 nm for all neutralization levels. Unfortunately, the similarity of the model predictions prevents determination of which model of ionomer morphology is correct based solely on the HVEM data. However, the spherical shape of the aggregates does

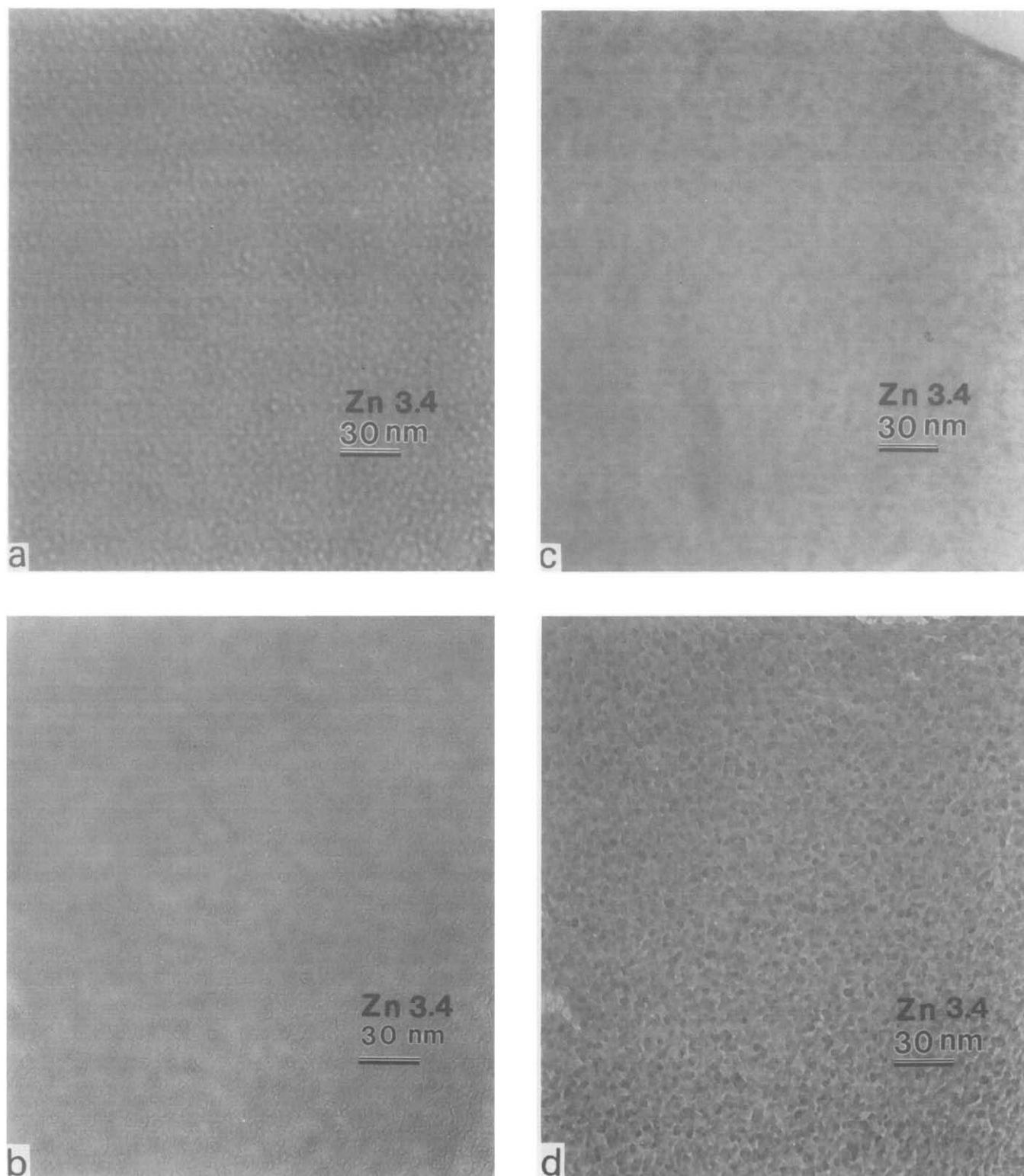


Figure 4 Zn^{2+} neutralized SPS, 3.37 mol% sulphonation, 30 μm aperture. (a) 20000 nm over focus; (b) 6000 nm over focus; (c) critical focus; (d) 500 nm under focus. The featureless spot visible at the top of (a), (c), and (d) is a hole in the film

indicate that a lamellar model of the ionic aggregates⁵ is inappropriate for these materials.

The diameters observed here are somewhat larger than those determined by SAXS modelling of bulk material (3 vs 2 nm), which may reflect the diminished constraints on polymer chains near a surface. A recent study of crazing in polystyrene homopolymer by low-angle electron diffraction³⁵ has shown that coarsening of the fibrils occurs at r.t., even though the glass transition of bulk polystyrene is

approximately 100°C. At 60°C, the process occurred within minutes. This demonstrates that when polymer chains are near a free surface, as in small diameter fibrils or ultra thin films, their mobility is enhanced. Because the size of the ionic aggregates in an ionomer will be determined by the balance between enthalpic and entropic forces², reducing the constraints on the polymer chains could allow the formation of larger ionic aggregates.

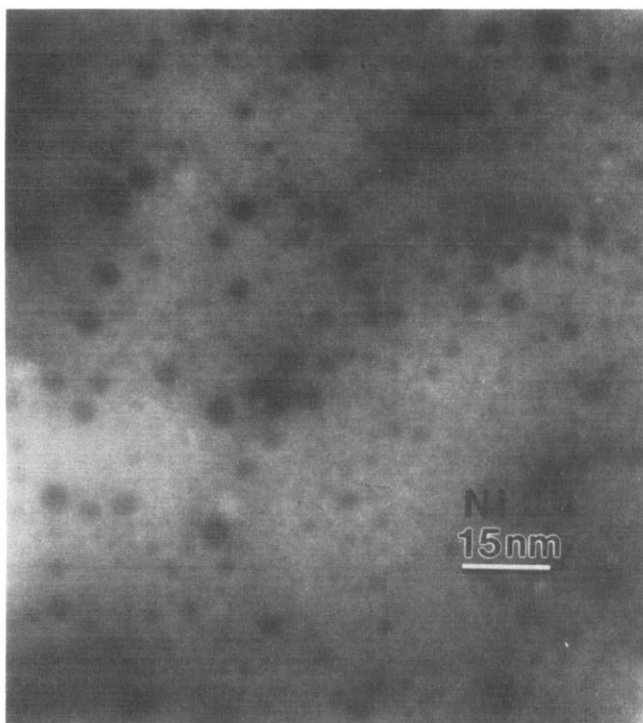


Figure 5 Ni²⁺ neutralized SPS, 3.37 mol% sulphonation, 10 μm aperture, critical focus. Note scale

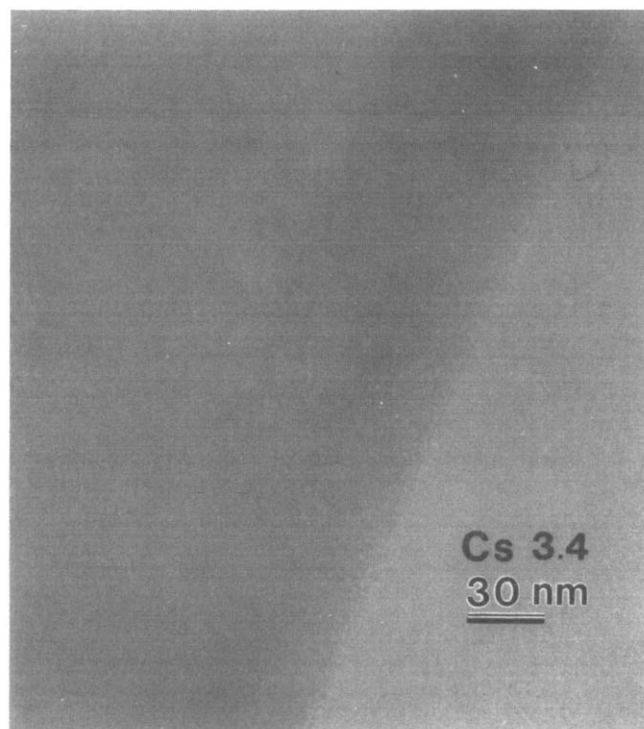


Figure 7 Cs⁺ neutralized SPS, 3.37 mol% sulphonation, 30 μm aperture, critical focus. The line running from top to bottom is the edge of the film; specimen is to the left

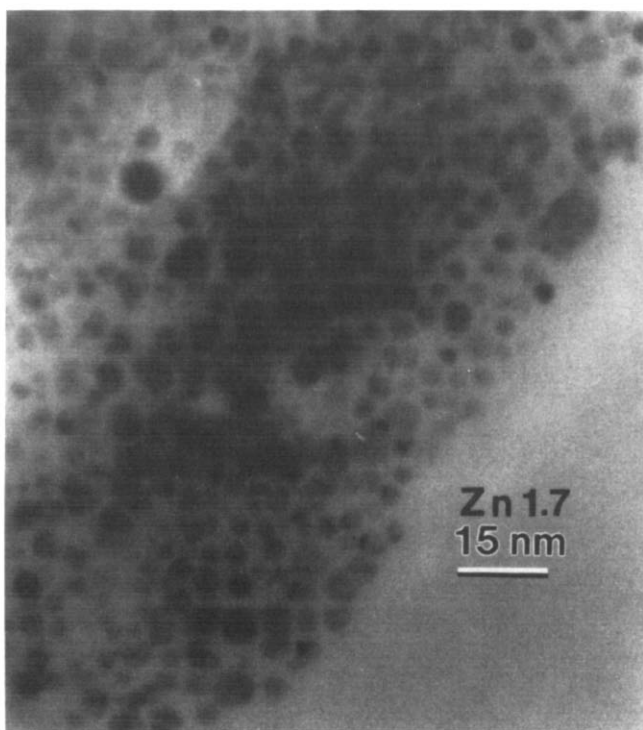


Figure 6 Zn²⁺ neutralized SPS, 1.68 mol% sulphonation, 10 μm aperture, critical focus. Note scale. The featureless region in the lower right corner is beyond the edge of the film

Comparing *Figures 4–6*, the dimensions of the ionic aggregates do not appear to change substantially when a different divalent neutralizing cation or a different sulphonation level is examined. This is consistent with the previous results of Yarusso⁷ for SAXS modelling of bulk SPS samples and with recent studies of sulphonated

polyurethane ionomers³⁶. A more interesting question is why no aggregates are observed in the Cs⁺ neutralized specimen of *Figure 7*. Based solely upon amplitude contrast, the Cs⁺ material should be easier to study because the atomic number of Cs (55) is nearly twice that of Ni (28) or Zn (30). In addition, because Cs⁺ is monovalent while Ni²⁺ and Zn²⁺ are divalent, the cation number density in the Cs⁺ neutralized sample is nearly twice that in the Ni²⁺ and Zn²⁺ neutralized specimens. Therefore, the results indicate that the Cs⁺ sample exhibits poor phase separation, reflecting a low degree of ionic aggregation.

In recent studies of Cs⁺ neutralized sulphonated polyurethane ionomers³⁶, both the electron density difference from SAXS modelling and the local structure as observed by extended X-ray absorption fine structure spectroscopy (EXAFS) indicate that the aggregates are poorly ordered. This may relate to the small charge to ionic radius ratio³⁷ of Cs⁺ (0.60 Å⁻¹) when compared with Ni²⁺ (2.90 Å⁻¹) or Zn²⁺ (2.70 Å⁻¹). In any case, if the aggregates are loosely packed in bulk, it is conceivable that with the rapid solvent evaporation used here, the CsSO₃ groups did not have sufficient time to aggregate and were effectively locked into the matrix. Such a phenomenon has been observed recently in Mn²⁺ neutralized SPS rapidly cast from tetrahydrofuran/water solution^{10,14}, where no SAXS peak was observable in the as-cast sample. In contrast to that study¹⁴, it was not possible to anneal the Cs⁺ neutralized ionomer film studied here in order to develop the ionic aggregates because surface tension forces in such thin films cause them to collapse.

CONCLUSIONS

Ionic domains were observed directly for the first time in

samples of Zn^{2+} and Ni^{2+} neutralized SPS, at sulphonation levels of 1.68 and 3.37 mol%, by using HVEM. The materials were rapidly cast from solution onto TEM grids to produce films of irregular thickness which contained 'thin spots' only a few interaggregate spacings thick, which allowed projection of an interpretable image in two dimensions. Through-focus series of the Zn^{2+} ionomer and of polystyrene homopolymer demonstrate that the observed contrast is not due to phase grain artifact. The aggregates were approximately 3 nm in diameter, in rough agreement with previous SAXS modelling (2 nm). The discrepancy could be due to the extreme thinness of the films observed here, perhaps allowing the formation of larger aggregates. No discernable differences were present between the different sulphonation levels or between the Zn^{2+} and Ni^{2+} samples. However, the Cs^+ neutralized material exhibited no ionic aggregates, despite the expected higher amplitude contrast. This is probably due to the rapid rate of solvent evaporation and weaker coulombic forces in the Cs^+ neutralized material, both of which hinder the formation of aggregates.

ACKNOWLEDGEMENTS

The authors thank the staff of the NIH Integrated Microscopy Resource at the University of Wisconsin at Madison for microscope access and training. In this regard, special thanks are due to Drs James B. Pawley and Peter H. Cooke. This work was supported in part by the Office of Naval Research through Grant N00014-83-K0423 and the Division of Materials Research of the National Science Foundation through Grant DMR-86-03839. R.A.R. wishes to thank the Fannie and John Hertz Foundation for support while this work was performed.

REFERENCES

- Eisenberg, A. and King, M. 'Ion Containing Polymers', Halsted-Wiley, New York (1975)
- Eisenberg, A. *Macromolecules* 1970, **3**, 147
- Wilson, F. C., Longworth, R. and Vaughan, D. *Polym. Prepr. (ACS Div. Polym. Chem.)* 1968, **9**, 505
- MacKnight, W. J., Taggart, W. P. and Stein, R. S. *J. Polym. Sci., Polym. Symp.* 1974, **45**, 113
- Roche, E. J., Stein, R. S., Russell, T. P. and MacKnight, W. J. *J. Polym. Sci., Polym. Phys. Edn.* 1980, **18**, 1497
- Gierke, T. D., Munn, G. E. and Wilson, F. C. *J. Polym. Sci., Polym. Phys. Edn.* 1981, **19**, 1687
- Yarusso, D. J. and Cooper, S. L. *Macromolecules* 1983, **16**, 1871
- Yarusso, D. J. and Cooper, S. L. *Polymer* 1985, **26**, 371
- Weiss, R. A. and Lefelar, J. *Polymer* 1986, **27**, 3
- Fitzgerald, J. J., Kim, D. and Weiss, R. A. *J. Polym. Sci., Polym. Lett. Edn.* 1986, **24**, 263
- Gebel, G., Aldebert, P. and Pinéri, M. *Macromolecules* 1987, **20**, 1428
- Fujimura, M., Hashimoto, T. and Kawai, H. *Macromolecules* 1981, **14**, 1309
- Fujimura, M., Hashimoto, T. and Kawai, H. *Macromolecules* 1982, **15**, 136
- Galambos, A. F., Stockton, W. B., Koberstein, J. T., Sen, A., Weiss, R. A. and Russell, T. P. *Macromolecules* 1987, **20**, 3091
- Roche, E. J., Stein, R. S. and MacKnight, W. J. *J. Polym. Sci., Polym. Phys. Edn.* 1980, **18**, 1035
- Roche, E. J., Pinéri, M., Duplessix, R. and Levelut, A. M. *J. Polym. Sci., Polym. Phys. Edn.* 1981, **19**, 1
- Earnest, T. R., Higgins, J. S. and MacKnight, W. J. *Macromolecules* 1982, **15**, 1390
- Clough, S. B., Cortelek, D., Nagabhushanam, T., Salamone, J. C. and Watterson, A. C. *Polym. Eng. Sci.* 1984, **24**, 385
- Handlin, D. L., MacKnight, W. J. and Thomas, E. L. *Macromolecules* 1981, **14**, 795
- Cowie, J. M. G. in 'Developments in Block Copolymers—1', (Ed. I. Goodman), Applied Science, New York (1982), 1
- Graiver, D., Litt, M. and Baer, E. *J. Polym. Sci., Polym. Chem. Edn.* 1979, **21**, 3573
- Graiver, D., Litt, M. and Baer, E. *J. Polym. Sci., Polym. Chem. Edn.* 1979, **21**, 3625
- Feng, D., Venkateshwaran, L., Wilkes, G. L., Leir, C. M. and Stark, J. E. *ACS Div. Polym. Mat. Sci. Eng. Prepr.* 1988, **58**, 999
- Handlin, D. L. and Thomas, E. L. *Macromolecules* 1983, **16**, 1514
- Marx, C. L., Koutsky, J. A. and Cooper, S. L. *Polym. Lett.* 1971, **9**, 167
- Phillips, P. J. *Polym. Lett.* 1972, **10**, 443
- Hsu, W. Y. and Gierke, T. D. *J. Membrane Sci.* 1983, **13**, 307
- Agarwal, P. K. and Prestridge, E. B. *Polymer* 1983, **24**, 487
- Pinéri, M., Meyer, C. and Bourret, A. *J. Polym. Sci., Polym. Phys. Edn.* 1975, **13**, 1881
- Meyer, C. T. and Pinéri, M. *J. Polym. Sci., Polym. Phys. Edn.* 1978, **16**, 569
- Makowski, H. S., Lundberg, R. D. and Singhal, G. H. *US Patent 3 870 841* granted March 11, 1975, assigned to Exxon Research and Engineering Company
- Siebourg, W., Lundberg, R. D. and Lenz, R. W. *Macromolecules* 1980, **13**, 1013
- Lundberg, R. D. and Makowski, H. S. in 'Ions in Polymers' (Ed. A. Eisenberg), *ACS Adv. Chem. Ser.* **187**, American Chemical Society, Washington DC (1980), 21
- Pawley, J. B. *Ultramicroscopy* 1984, **13**, 387
- Yang, A. C.-m. and Kramer, E. J. *J. Polym. Sci., Polym. Phys. Edn.* 1985, **23**, 1353
- Ding, Y. S. *PhD Thesis*, University of Wisconsin at Madison, 1986
- Weast, R. C., Ed., 'CRC Handbook of Chemistry and Physics', 59th edn, CRC Press, West Palm Beach (1978)